

~~CONFIDENTIAL~~

Copy
RM L50F06

94

NACA RM L50F06

~~53-33-46~~

NACA

TECH LIBRARY KAFB, NM
0149809

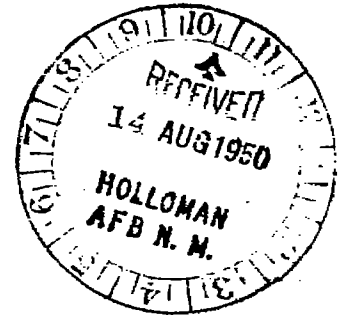
RESEARCH MEMORANDUM

PRESSURE MEASUREMENTS ON A SHARPLY CONVERGING
FUSELAGE AFTERBODY WITH JET ON AND OFF

AT MACH NUMBERS FROM 0.8 TO 1.6

By William E. Stoney, Jr. and Ellis Katz

Langley Aeronautical Laboratory
Langley Air Force Base, Va.



WES

~~This document contains classified information...
...the National Defense of the United States...
...USC 50 and 52. Its transmission or the
...revelation of its contents in any manner to an
...unauthorized person is prohibited by law.
...Information so classified shall be imparted
...only to persons in the Army and naval
...services of the United States, appropriate
...civilian officers and employees of the Federal
...Government who have a legitimate interest
...therein, and to United States citizens whose
...loyalty and discretion who of necessity must
...be informed thereof.~~

NATIONAL ADVISORY COMMITTEE
FOR AERONAUTICS

WASHINGTON
August 10, 1950

~~CONFIDENTIAL~~

207.7A/13

~~53-33-46~~

7197

Classification code of the record to Unclassified

By Authority of Nova Tech Pub Announcement #10-2

By 22 Jun 56

GRADE OF OFFICIAL MAKING CHANGE NK

5 Aug 61
DATE



NATIONAL ADVISORY COMMITTEE FOR AERONAUTICS

RESEARCH MEMORANDUM

PRESSURE MEASUREMENTS ON A SHARPLY CONVERGING
FUSELAGE AFTERBODY WITH JET ON AND OFF
AT MACH NUMBERS FROM 0.8 TO 1.6

By William E. Stoney, Jr. and Ellis Katz

SUMMARY

A rocket-powered model of a fin-stabilized parabolic body of revolution with fineness ratio 8.91 and maximum diameter located at the 80 percent body station was flown at Mach numbers from 0.8 to 1.6 to determine the static pressures at two orifices located rearward of the stabilizing fins at the 91.4 and the 99.6 percent stations along the body.

Both theory and experiment show that the suction and the drag over the afterbody were very high. At a Mach number of 1.4 the pressure coefficients at both orifices were more positive than those predicted by the Von Kármán-Moore theory. The pressure recovery at the rear of the body was indicated to be much greater than that shown by the theory. At subsonic speeds the agreement between theory and experiment was fair at both orifices. There were indications that the pressure drag over the afterbody was lower than that calculated by theory. At both supersonic and subsonic velocities the jet raised the pressure at the rear orifice considerably, while its effect on the forward orifice was restricted to subsonic Mach numbers.

INTRODUCTION

In flight tests conducted by the NACA on bodies of revolution differing in fineness ratio and position of maximum diameter, it was noted (reference 1) that the drag of bodies having sharply converging afterbodies, although high, was significantly lower than that indicated by the Von Kármán-Moore linearized theory. The present investigation was carried out to investigate this phenomenon and to help clarify the nature of the flow over bodies having sharply converging afterbodies.

As the linearized theory might naturally be expected to be in greatest error over the rapidly converging afterbody, two pressures were measured which were expected to be indicative of the flow over the afterbody.

The test was performed on a rocket-propelled body at the Pilotless Aircraft Research Station at Wallops Island, Va. The fin-stabilized body was of 8.91 fineness ratio and had its maximum diameter located at 80 percent of the body length.

The Mach number range of 0.8 to 1.65 corresponds to a Reynolds number range of 23×10^6 to 63×10^6 based on body length.

SYMBOLS

C_D	drag coefficient based on body frontal area of 0.307 square foot
C_p	pressure coefficient $\left(\frac{p - p_0}{\frac{1}{2}\rho V^2} \right)$
p	static pressure at orifice, pounds per square foot
p_0	free-stream static pressure, pounds per square foot
ρ	free-stream density, slugs per cubic foot
V	true airspeed, feet per second
M	Mach number
R	Reynolds number based on body length of 5.56 feet
R_m	maximum radius of body, 0.312 foot
L	body length, 5.56 feet
r	body radius at station x
x	distance along body measured from nose
$B = \sqrt{M^2 - 1}$	

MODEL AND TEST

The general arrangement and photographs of the test configuration are shown in figures 1 and 2. The profile of the body described parabolic arcs, the equations of which are as follows:

For $0 \leq \frac{x}{L} \leq 0.8$,

$$\frac{r}{R_m} = 1 - 1.561 \left(0.8 - \frac{x}{L}\right)^2$$

For $0.8 \leq \frac{x}{L} \leq 1$

$$\frac{r}{R_m} = 1 - 14.063 \left(\frac{x}{L} - 0.8\right)^2$$

where R_m is the maximum radius and L is the total length.

The model was 5.56 feet long and had a frontal area (πR_m^2) of 0.307 square foot and a base area of 0.0586 square foot. The body was constructed of wood and finished with clear lacquer to form a smooth and fair surface.

The test vehicle was stabilized by three dural fins, swept back 45° and having 1.69 square feet total exposed area. In the streamwise direction the fins had hexagonal sections of 0.0278 thickness ratio. The trailing edge of the fins intersected the body at the 90.53 percent station.

A two-stage propulsion system was employed utilizing a shortened 3.25-inch Mk.7 rocket motor as the sustainer unit and a modified light-weight 5-inch HVAR motor as the booster unit. The booster unit was stabilized by four fins and was attached to the sustainer motor by means of a nozzle-plug adapter.

The model was fired at an angle of 55° to the horizontal. Test data were obtained and reduced by the methods described in reference 2. Drag coefficients have been based on body frontal area (0.307 sq ft) and represent the total drag of the configuration including fin and interference drag.

The model was equipped with a two-channel telemeter for recording the static pressure at two body orifices. Both orifices were $3/16$ inch

in diameter. The estimated maximum systematic errors in drag and pressure coefficients at various Mach numbers are as follows:

Mach numbers	C_D	C_p front	C_p rear
0.80	± 0.025	± 0.069	± 0.080
1.10	± 0.014	± 0.024	± 0.034
1.40	± 0.019	± 0.014	± 0.015

Experience indicates that the maximum systematic error in Mach number is ± 0.010 over the Mach number range tested.

In figure 3, the Reynolds number during flight, based on body length, is plotted against Mach number.

THEORETICAL CALCULATIONS

In this paper, mention is frequently made of various theoretical calculations and plots. The theoretical methods used were chosen for comparison with the experimental results because it was felt they embodied a reasonable degree of accuracy while still retaining an ease of computation suitable for practical use. The incompressible pressure distribution was computed by extending the rear of the body to its center line and using the method of Von Kármán (reference 3), wherein the body is divided at its maximum diameter and the pressures calculated for each isolated half. This simplification causes a discontinuity in the subsonic pressure curve; however, it is believed that the pressures over most of the body are unaffected by the approximations in this method. The variation of the pressure coefficient with subsonic Mach numbers was calculated by the method derived by Lester Lees (reference 4) for ellipsoids. Reference 5 compares this method with experimental results for several nonellipsoid bodies, with good agreement. The linearized method of Von Kármán and Moore (reference 6) was used to compute the pressure distribution at $M = 1.4$. The variation of pressure coefficient with supersonic Mach number was calculated using the experimental pressure coefficient at $M = 1.4$ and the simplified method proposed by Laitone in reference 7. All calculations were made for jet-off flight.

RESULTS AND DISCUSSION

Measured Pressures

The pressures measured on the afterbody are presented in figure 4 as pressure coefficient C_p against Mach number M . The results are presented for power-on and power-off conditions.

Power-off flight.- The forward orifice was located at approximately the station where the drag contribution was calculated to be greatest and showed very large suction throughout the test range. It may be noted here that the suction is of a greater magnitude than those measured on the bases of square-end bodies of revolution (reference 8). The rear orifice, located as near the 100 percent station as practical, showed positive pressure coefficients over most of the Mach number range.

The sharp transition at the forward orifice at $M = 0.92$ is indicated to be coincident with the local pressure reaching a critical value corresponding to a local Mach number of 1.00. A similar transition at $M = 0.92$ is not observed for the jet-on flight; however, the influence of the jet may have caused large entropy changes during power-on flight.

Although the nature of the oscillations observed in the pressures at the forward orifice during unpowered flight from about $M = 1.30$ to $M = 1.63$ is not understood, it is believed that these variations are the result of aerodynamic phenomena and are not products of the pressure-measuring system.

Power-on flight.- The curves for power-on flight show that the effect of the jet was negligible on the pressures at the forward orifice at supersonic speeds and was considerable on the pressure at the rear orifice. The higher pressures at the rear orifice during power-on flight indicate a favorable effect of the jet on drag. A similar observation was made in reference 9 on the effect of an underexpanded jet on pressures on a converging afterbody. These higher pressures at the rear orifice are probably due in part to the effect of the high jet pressures being transmitted forward in the boundary layer. This favorable effect on over-all drag is probably greatest at subsonic Mach numbers since the power-on pressures for the front orifice are also much higher in this range. It should be mentioned, however, that the preceding results are applicable only to the present test body and jet characteristics. For reference purposes, it is noted here that the 3.25-inch sustainer rocket motor used had an underexpanded nozzle, which had an exit static pressure of about 28 pounds per square inch absolute,

and an exit velocity of about 6200 feet per second which corresponds to an exit Mach number of 2.6. The average atmospheric static pressure during thrusting flight was 14.1 pounds per square inch. The nozzle exit conditions at burnout have been observed from flight and ground tests to change abruptly from an underexpanded to an overexpanded flow as the thrust drops to zero. This rapid fluctuation in nozzle exit pressure is seen to have caused a pronounced reduction of the pressures at the rear orifice near $M = 1.63$. This same effect of overexpansion is noted for power-off flight between $M = 1.64$ and $M = 1.44$ where the pressures at this rear orifice are believed to be reduced due to a slight degree of rocket motor afterburning.

Comparison of Theory and Experiment

As is shown in figure 4, the agreement of the subsonic theory with the test values is fairly good although the incompressible theory has not been corrected for the presence of the flat base. The subsonic variation of C_p with Mach number as calculated by the method of Lees (reference 4) agrees well with that of the test at both orifices. The variation of C_p with supersonic Mach number as calculated by the method of Laitone (reference 7) was less than that shown by the test results at both orifices.

Figure 5 shows the pressure profiles for the test model, calculated by the methods described in the section on theoretical calculations.

Both the subsonic and supersonic theories predict large suction followed by rapid recompression over the afterbody; the experimental results indicate the same variation, except that the recompression is indicated to be of much greater magnitude than calculated. The large pressure recovery between the forward and rear orifice indicates that little or no flow separation occurred over the afterbody. This is in agreement with the observations of Chapman and Perkins in reference 10, wherein they showed no separation for turbulent flow over similarly converging afterbodies.

Figure 6 is a plot of the pressure-drag distribution over the body length at $M = 1.4$. This curve was calculated from the Von Kármán-Moore pressure distribution by use of the following formula:

$$\frac{dC_D}{d\left(\frac{x}{L}\right)} = \frac{2L}{R_m^2} C_{p^*} \frac{dr}{dx}$$

Also shown in figure 6 are the experimental values calculated from the measured pressures. Both theory and experiment show that the afterbody had very high pressure drag. The experimental points show that, at the orifice locations, the drag contribution was lower than calculated over the afterbody without fins.

Drag

The variation of the total power-off drag coefficient with Mach number for the test model and for two identical models (taken from reference 11) is presented in figure 7. It is interesting to note that the steep drag rise and the decreasing drag coefficients in the supersonic range were similar to the pressure variation shown in figure 4 for the forward orifice. It may also be mentioned that the variation is characteristic for parabolic bodies of revolution having extreme rearward locations of maximum diameter as was shown in reference 11.

Also shown in figure 7 is a breakdown of the components of drag at $M = 1.4$. The isolated fin drag was measured in flight on a cylindrical body by use of the technique described in reference 2; the base drag was estimated from unpublished data for a series of bodies having converging afterbodies; the friction drag was estimated using an average friction coefficient of 0.002 (based on wetted area); and the pressure drag was taken from the following table, which was derived from the calculated drag distribution of figure 6 and gives the increment of pressure drag contributed by each section of the body:

	ΔC_D
Forebody	0.0268
Afterbody	0.1840
Total	0.2108

Although the breakdown of total drag is not intended to be rigorous, it is believed that it indicates the calculated pressure-drag contribution of the afterbody to be too great as the calculated drag components presented are the minimum reasonable values and the pressure drag is 65 percent of the total drag. This indication is supported by the observations noted in figure 6 wherein the measured drag contributions at the orifice locations were found to be less than calculated. It should be noted here that the theoretical calculations neglected the effect of the fins on the body.

CONCLUSIONS

A flight test was performed on a fin-stabilized body of revolution to determine the nature of the pressure forces acting over the rear portion of the body. Within the limits of the test, the following effects were noted:

1. Both theory and experiment show that the drag of the afterbody was very high due to extreme suction over that section of the body.

2. At a Mach number of 1.4, the pressure coefficients at 91.1 and 99.6 percent body stations were more positive than those predicted by the Von Kármán-Moore theory. The pressure recovery over the afterbody was indicated to be much greater than shown by the Von Kármán-Moore theory. The supersonic variation of C_p with Mach number as calculated by the method of Laitone was less than that shown by the test results. The incompressible potential theory corrected for compressibility effects showed fair agreement with the experimental pressures at subsonic speeds.

3. There were indications that the pressure drag over the afterbody was lower than that calculated by theory.

4. At supersonic and subsonic speeds the jet raised the pressure at the rear orifice considerably, while its effect on the forward orifice was restricted to subsonic Mach numbers.

Langley Aeronautical Laboratory
National Advisory Committee for Aeronautics
Langley Air Force Base, Va.

REFERENCES

1. Katz, Ellis R.: Flight Investigation at High-Subsonic, Transonic, and Supersonic Speeds to Determine Zero-Lift Drag of Bodies of Revolution Having Fineness Ratio of 6.04 and Varying Positions of Maximum Diameter. NACA RM L9F02, 1949.
2. Morrow, John D., and Katz, Ellis: Flight Investigation at Mach Numbers from 0.6 to 1.7 to Determine Drag and Base Pressures on a Blunt-Trailing-Edge Airfoil and Drag of Diamond and Circular-Arc Airfoils at Zero Lift. NACA RM L50E19a, 1950.
3. Von Kármán, Theodor: Calculation of Pressure Distribution on Airship Hulls. NACA TM 574, 1930.
4. Lees, Lester: A Discussion of the Application of the Prandtl-Glauert Method to Subsonic Compressible Flow over a Slender Body of Revolution. NACA TN 1127, 1946.
5. Matthews, Clarence W.: A Comparison of the Experimental Subsonic Pressure Distributions about Several Bodies of Revolution with Pressure Distributions Computed by Means of the Linearized Theory. NACA RM L9F28, 1949.
6. Von Kármán, Theodor, and Moore, Norton B.: Resistance of Slender Bodies Moving with Supersonic Velocities with Special Reference to Projectiles. Trans. A.S.M.E., vol. 54, no. 23, Dec. 15, 1932, pp. 303-310.
7. Laitone, E. V.: The Linearized Subsonic and Supersonic Flow about Inclined Slender Bodies of Revolution. Jour. Aero. Sci., vol. 14, no. 11, Nov. 1947, pp. 631-642.
8. Faro, I. D. V.: Experimental Determination of Base Pressures at Supersonic Velocities. Bumblebee Rep. No. 106, The Johns Hopkins Univ., Appl. Phys. Lab., Nov. 1949.
9. Love, Eugene S.: Aerodynamic Investigation of a Parabolic Body of Revolution at Mach Number of 1.92 and Some Effects of an Annular Jet Exhausting from the Base. NACA RM L9K09, 1950.
10. Chapman, Dean R., and Perkins, Edward W.: Experimental Investigation of the Effects of Viscosity on the Drag of Bodies of Revolution at a Mach Number of 1.5. NACA RM A7A31a, 1947.

11. Hart, Roger G., and Katz, Ellis R.: Flight Investigations at High-Subsonic, Transonic, and Supersonic Speeds to Determine Zero-Lift Drag of Fin-Stabilized Bodies of Revolution Having Fineness Ratios of 12.5, 8.91, and 6.04 and Varying Positions of Maximum Diameter. NACA RM L9I30, 1949.

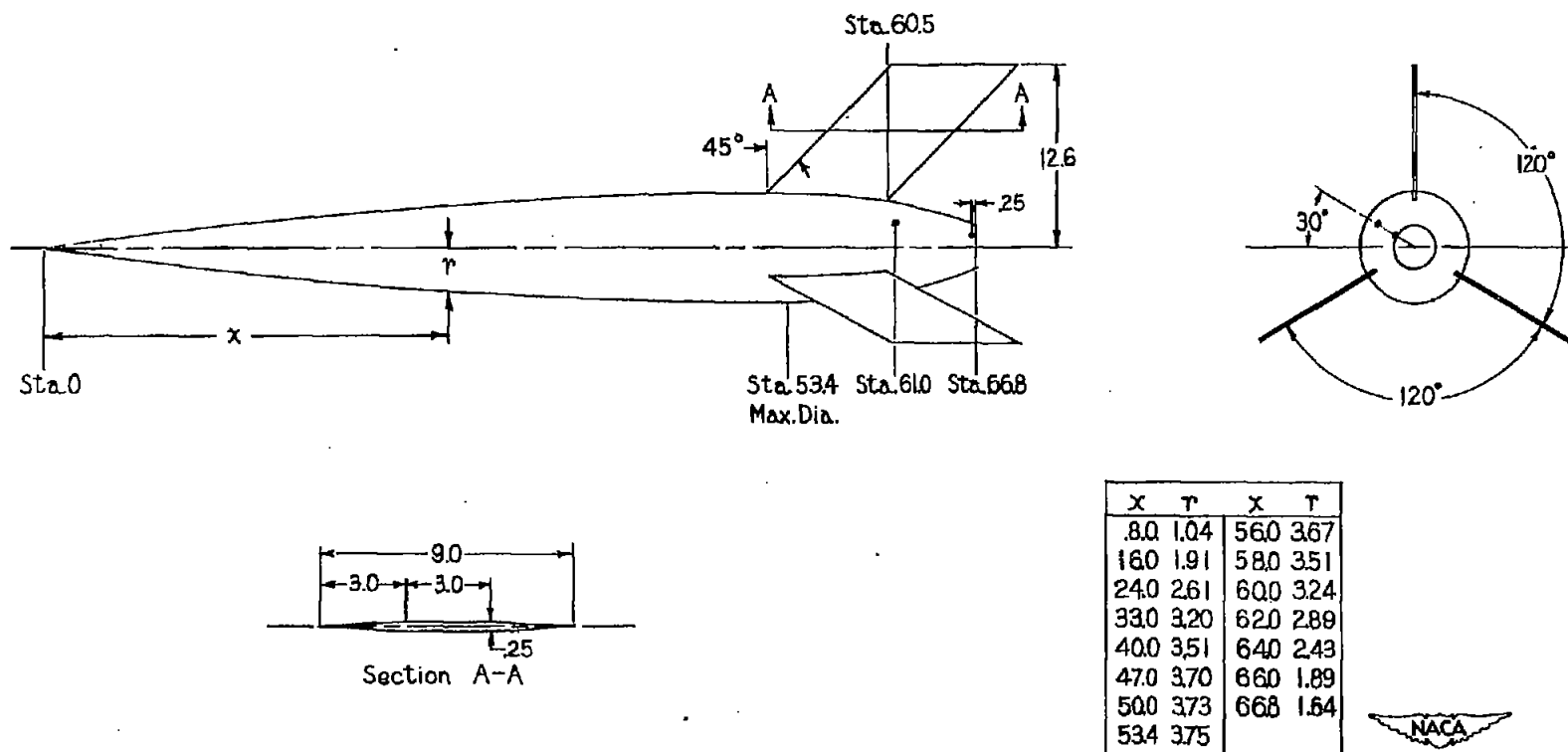


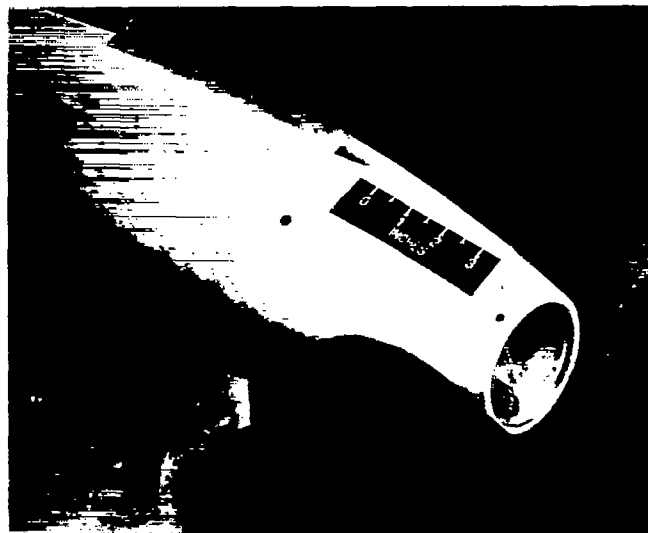
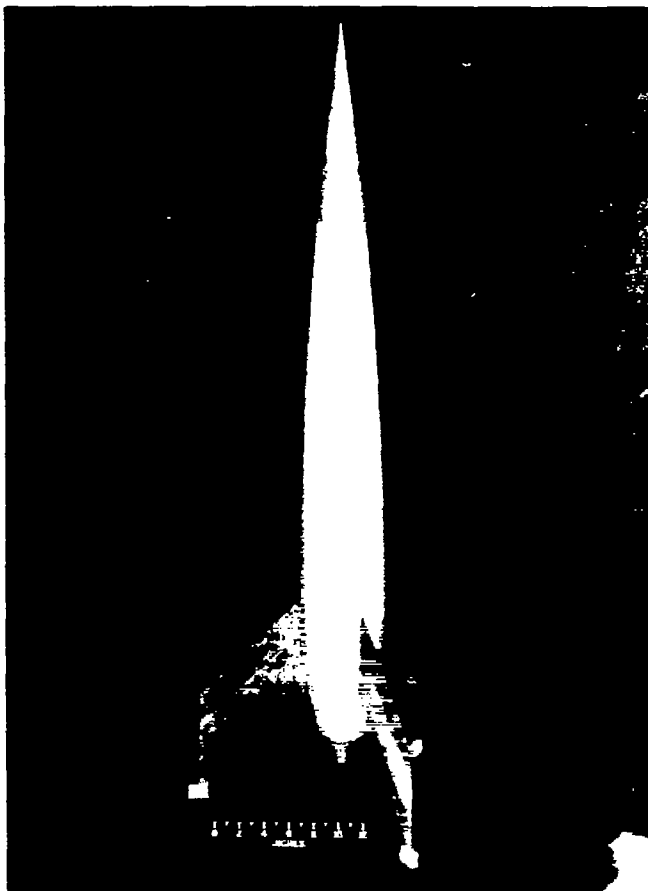
Figure 1.- General arrangement of test vehicle showing location of pressure orifices. (All dimensions in inches.)

1

2

3

4



NACA
L-64890

Figure 2.- General and detail views of the test vehicle showing the location of the two pressure orifices.

•
•

•
•

•
•

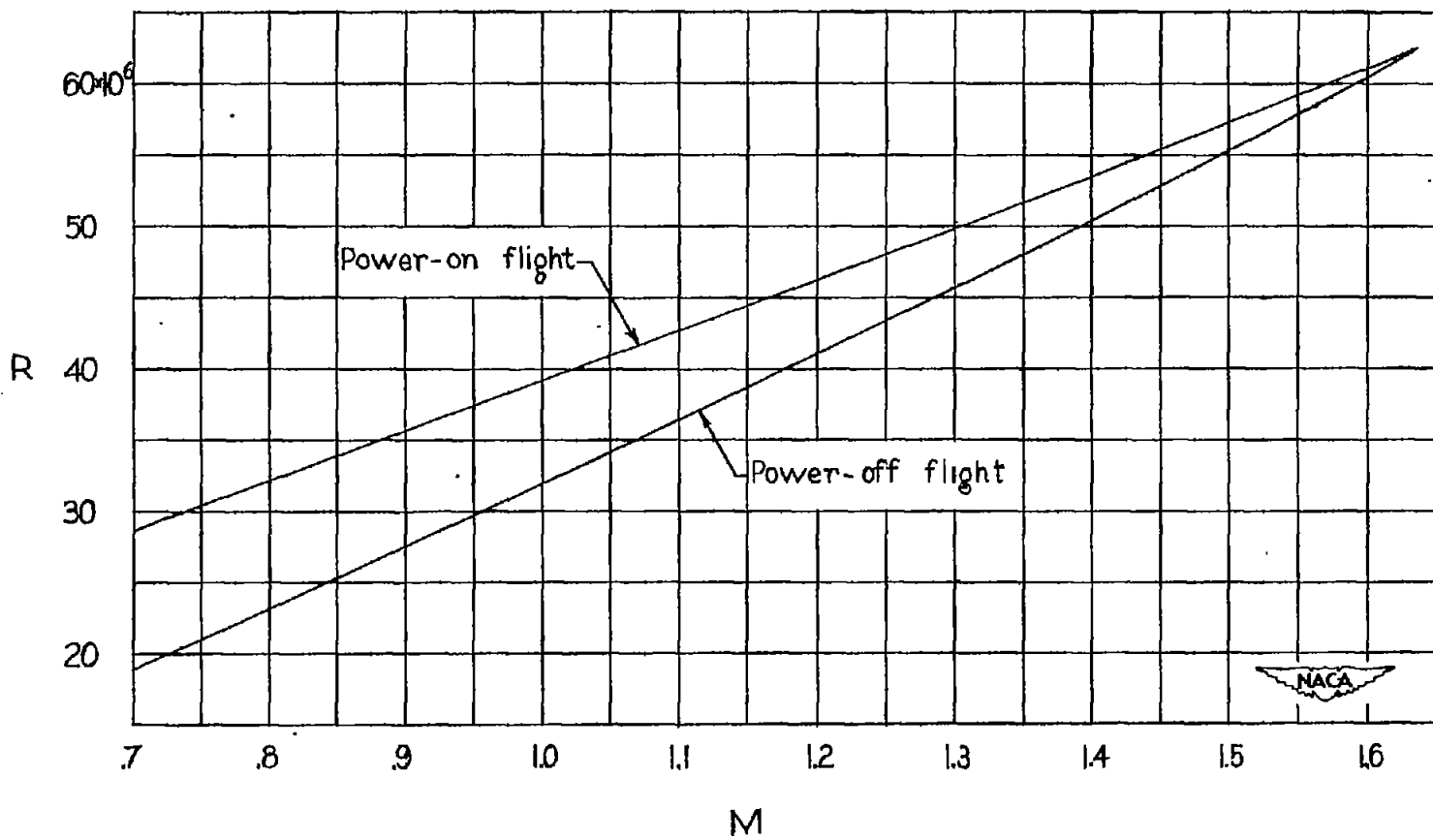


Figure 3.- Reynolds number based on body length against Mach number.

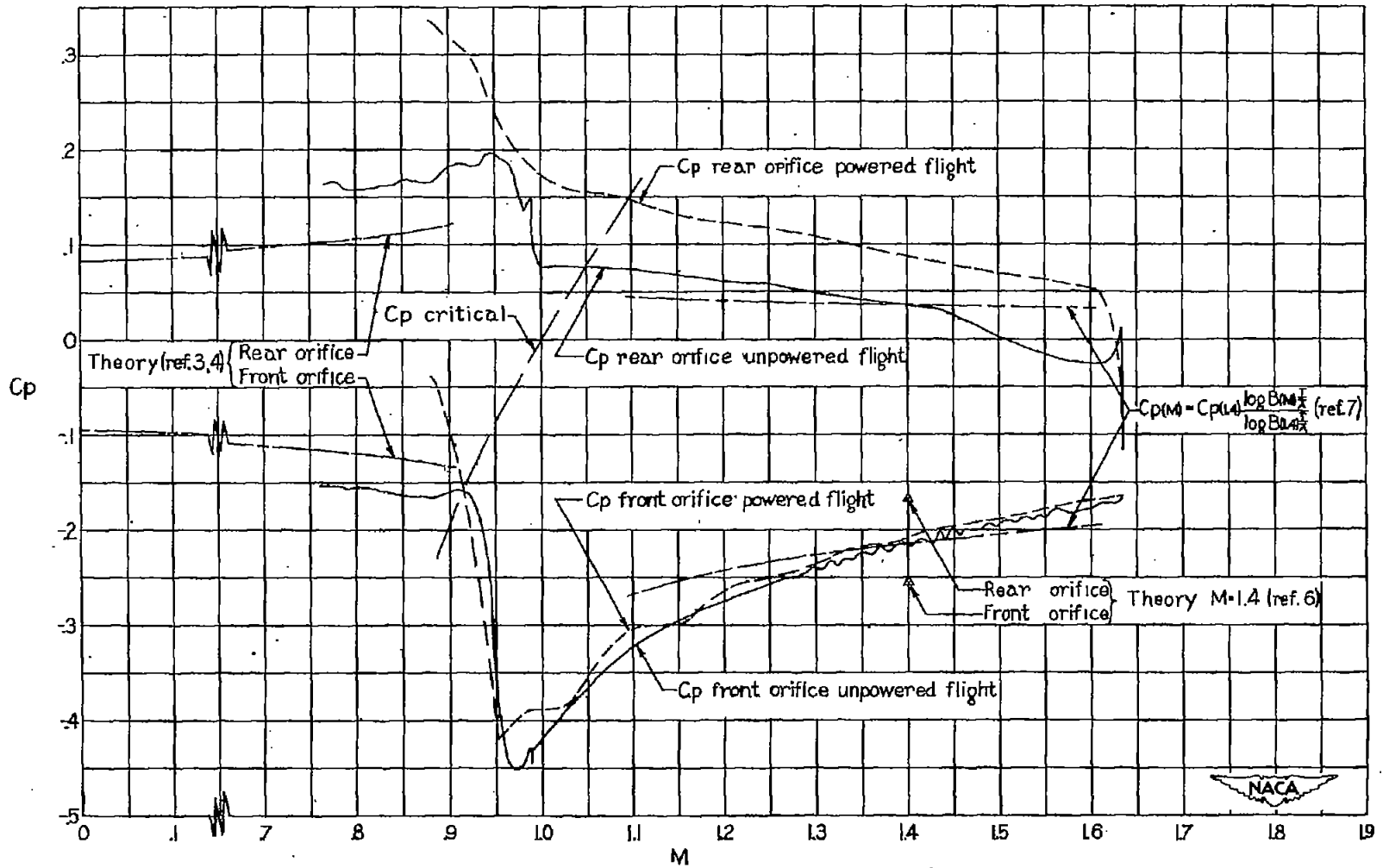


Figure 4.- Pressure coefficients with power on and off for both orifices against Mach number.

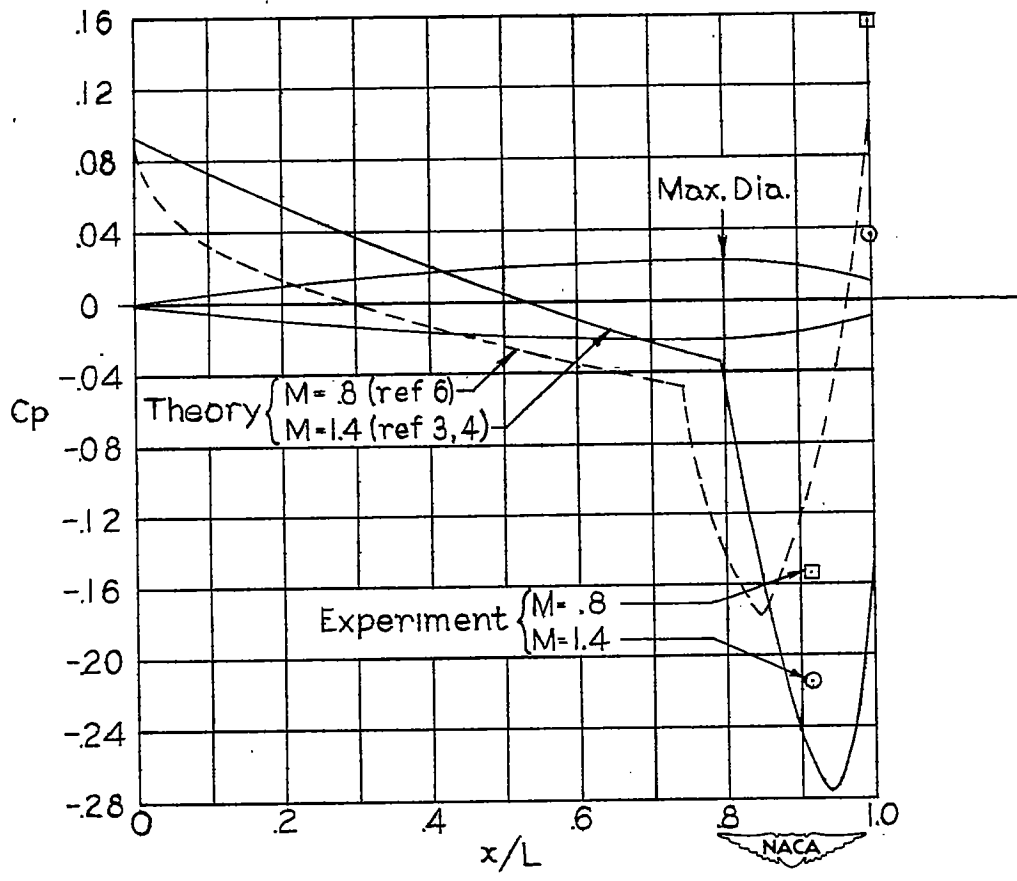


Figure 5.- Pressure coefficient C_p against x/L .

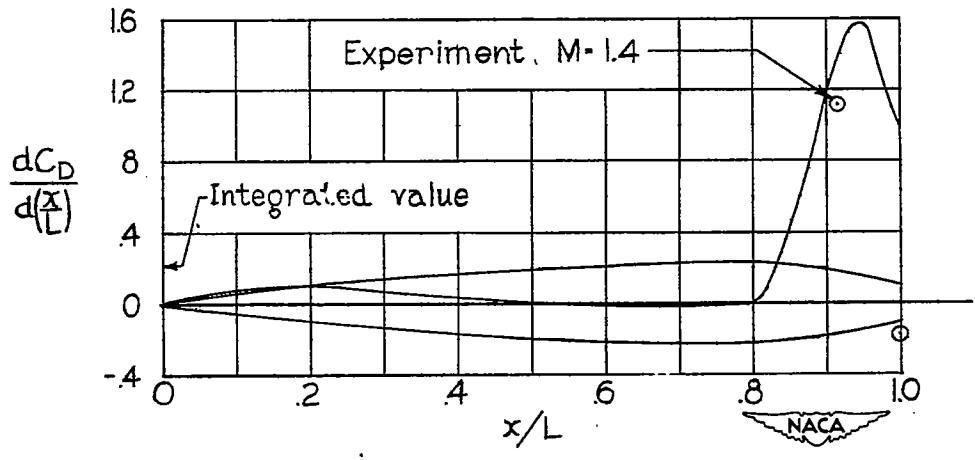


Figure 6.- Pressure drag distribution at $M = 1.4$.

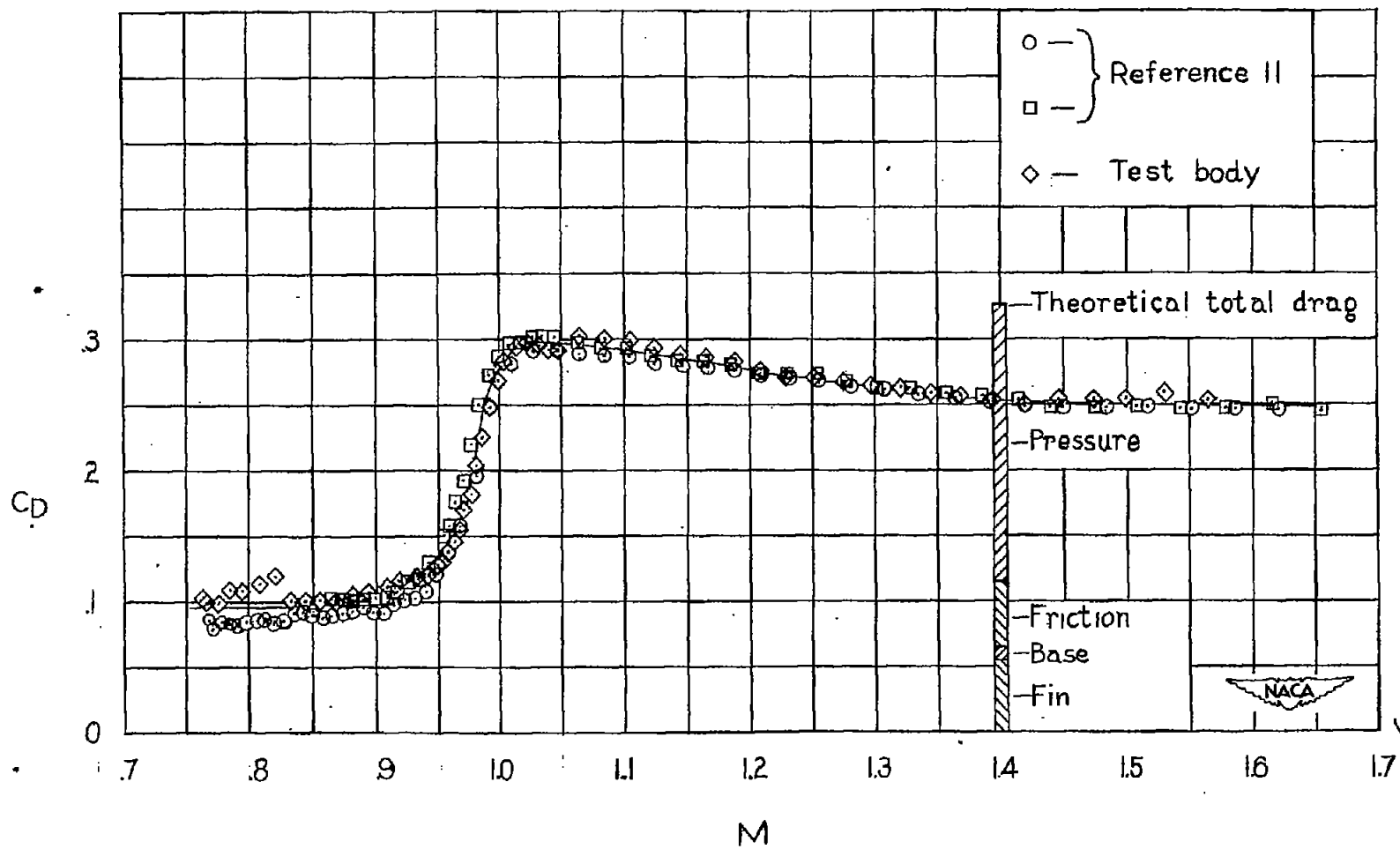


Figure 7.- Power-off drag coefficient against Mach number for three identical configurations.